

# Gulf Stream Surface Transport and Statistics at 69°W from the Geosat Altimeter

KATHRYN A. KELLY AND SARAH T. GILLE

*Woods Hole Oceanographic Institution, Woods Hole, Massachusetts*

Geosat altimeter height measurements for the Gulf Stream for three subtracks from the Exact Repeat Mission were processed to remove the geoid and mean Gulf Stream height. A Gaussian model for the Gulf Stream velocity profile was used to predict the form of the residual height profiles seen by Geosat and the mean height profile, using estimates of the width and position derived from the height residuals. Estimates of the maximum surface velocity and the surface transport were obtained by a least squares fit of the synthetic height profiles to the data. Location statistics from the Geosat data were in good agreement with values obtained from infrared images of the Gulf Stream. Maximum surface velocities were typically between 1.2 and 2.0 m s<sup>-1</sup>. The time series showed that surface transport is correlated primarily with the magnitude of the surface velocities, although an anomalously large increase in surface transport in the winter of 1987-1988 was caused by an increase in the width of the Gulf Stream. An analysis of the average annual signal in transport showed maximum values in the late fall and minimum transport in the late spring. Maximum (minimum) surface transport generally occurred when the Gulf Stream was north (south) of its mean position.

## 1. INTRODUCTION

The Geosat altimeter Exact Repeat Mission, which measures collinear profiles of the sea surface height every 17 days, has produced a record of the Gulf Stream extending more than 2 years. Since the altimeter measures the absolute height of the sea surface, it is necessary to know the Earth's geoid and to make a series of other corrections to determine the dynamic topography (see, for example, *Calman, [1987]*). Because the geoid is not known on length scales comparable to oceanic mesoscale features, the variability of the height field has been used in most analyses of the data and in assimilation into numerical models [e.g., *Robinson and Walstad, 1987*]. Meanwhile, efforts have been made to measure the dynamic height along Geosat subtracks for comparison with the altimeter height in order to extract the alongtrack geoid [*Mitchell et al., 1987*].

We describe here an analysis of a portion of the Gulf Stream to demonstrate that the use of a simple model for the velocity profile can assist in determining Gulf Stream kinematics and in estimating the mean dynamic topography, which in turn leads to an estimate of the absolute surface geostrophic velocity and transport. Although the combination of ascending and descending subtracks could determine the two-dimensional structure of the dynamic height field, about half of the Geosat data along descending subtracks in the Gulf Stream region were unusable because of instrument problems. Fortunately, parallel ascending subtracks, 115 km apart and separated in time by about 3 days, intersect the Gulf Stream nearly at right angles to its mean path for much of its length, giving profiles across the Gulf Stream with 7.3-km alongtrack resolution (Plate 1). (Plate 1 is shown here in black and white. The color version can be found in the separate color section in this issue.) In the analysis presented here we have used only the ascending collinear

subtracks and based our model on the corresponding cross-stream height profile.

The justification for the model is described in section 2, followed by a description of the data processing in section 3. The procedures for estimating model parameters and for fitting the synthetic height profiles to the data and the critical issue of convergence of the iterative procedure are described in section 4, followed by error estimates and the time series of model parameters in section 5, along with comparisons of the results with other measurements in section 6. Conclusions follow in section 7.

## 2. A SIMPLE MODEL FOR THE VELOCITY PROFILE

Previous studies of the Gulf Stream velocity profile using acoustic Doppler current profiler (ADCP) [*Joyce et al., 1986*] and subsurface moorings [*Hall and Bryden, 1985*] have suggested that at least to first order, it has a Gaussian shape of the form

$$u(y) = a_1 \exp \left[ \frac{-(y - a_2)^2}{2a_3^2} \right] \quad (1)$$

where  $u$  is the (downstream) velocity as a function of (cross-stream) position  $y$ ,  $a_1$  is the velocity maximum,  $a_2$  is the position of the center of the Gulf Stream, and  $a_3$  is a width parameter corresponding to the standard deviation in the usual definition for a Gaussian distribution (Figure 1). The dynamic height profile relative to some reference level is then given by the integral of (1),

$$h(y) = -\frac{f}{g} \int u(y') dy' \quad (2)$$

Conversely, one could hypothetically find the velocity profile by differentiating the height profile from the Geosat altimeter; however only rarely does the Geosat subtrack intersect the Gulf Stream exactly perpendicular to the flow. Instead the Gulf Stream meanders some angle  $\theta$  from the line perpendicular to the ascending Geosat subtracks (Figure 1). While the crossing angle will have no effect on the measured height difference across the Gulf Stream, it does increase

Copyright 1990 by the American Geophysical Union.

Paper number 89JCO3118.

0148-0277/90/89JC-03118\$05.00

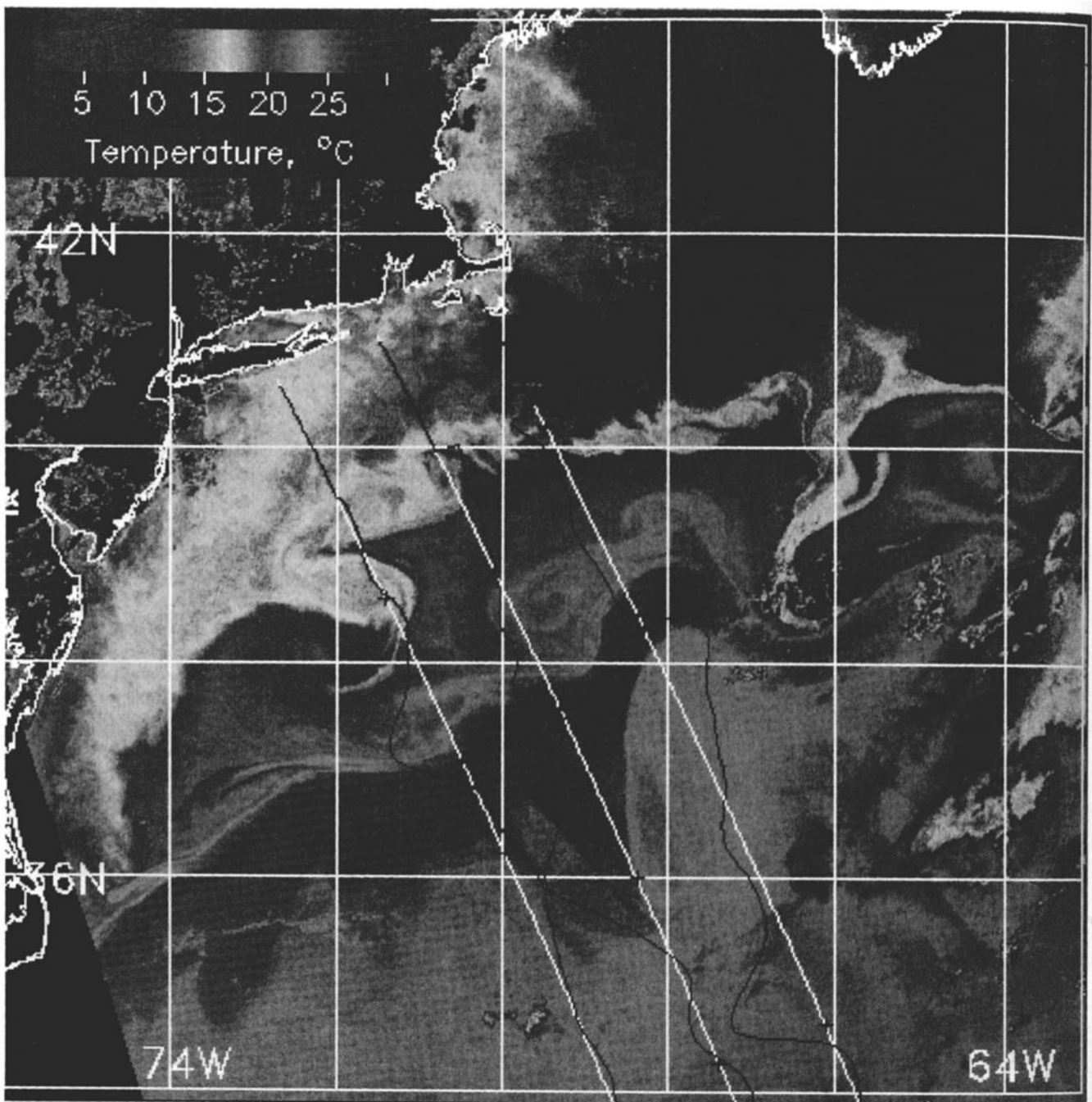


Plate 1. Geosat height residuals from the three subtracks used in this study superimposed on IR image (courtesy of National Marine Fisheries Service). The image is from day 151 of 1987, and the heights (from left to right) are for subtrack a002 on day 151, subtrack a045 on day 154, and subtrack a088 on day 157. The residuals are projected perpendicular to the tracks (positive to the right), and the relative maximum slopes are shown as crosses on the subtracks. The positions of three of the maximum slopes fall clearly within the Gulf Stream, as delineated by the warm water. (The color version and a complete description of this figure can be found in the separate color section in this issue.)

the alongtrack Gulf Stream width so that the cross-stream width parameter  $w$  is given in terms of the alongtrack width  $a_3$  and the crossing angle as

$$w = a_3 \cos \theta \quad (3)$$

The corresponding alongtrack velocity profile is smaller in amplitude than the downstream velocity because the derivative of height gives the velocity perpendicular to the subtrack. The maximum downstream velocity  $u_d$  can be written in terms of the crossing angle as

$$u_d = \frac{a_1}{\cos \theta} \quad (4)$$

The surface transport is proportional to the height difference across the stream and is independent of the crossing angle, that is,

$$\Delta h \propto a_1 a_3 = u_d w \quad (5)$$

The problem in using the altimeter data is that, in the absence of a detailed geoid, the average of collinear profiles must be subtracted to eliminate the larger geoid signal; this

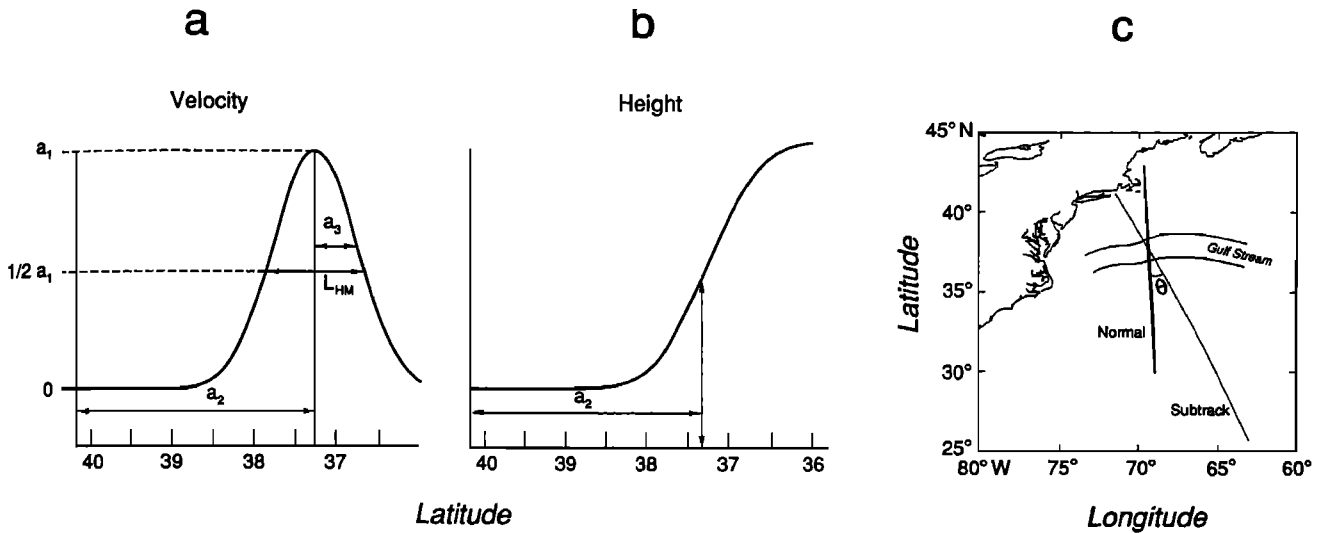


Fig. 1. Definition sketch of the Gulf Stream model. (a) The Gaussian velocity profile is characterized by the maximum velocity  $a_1$ , the position of the center  $a_2$ , and the width parameter  $a_3$ . (b) The sea surface height is obtained by integrating the velocity profile. The maximum slope corresponds to the center of the Gaussian profile. (c) The crossing angle  $\theta$  is the angle between the subtrack and a perpendicular to the Gulf Stream axis.

also removes the mean sea surface topography. Can one then infer some information about the position, width, and velocity of the Gulf Stream from the sea surface height residuals? And, having this information, can one estimate the mean height profiles along the subtracks?

To understand the effect of each of the parameters  $a_i$  on the mean and residual height profiles, synthetic velocity profiles were computed and integrated to produce height profiles as each of the three parameters was varied in turn, through a range of possible values. For each parameter, all of the height profiles were averaged, and the mean subtracted from each height profile to produce synthetic residual height

profiles (Figure 2). Since we expect the Gulf Stream to meander a distance comparable to its width downstream of Cape Hatteras [Cornillon, 1986], the fluctuating part of  $a_2$  was assumed to be relatively large. Thus the most significant effects were seen in varying  $a_2$ , the position parameter. These synthetic profiles were used as a guide for interpreting the actual data profiles. For example, when the Gulf Stream is significantly north of its mean position (Figure 2a), the residual height profile has a positive anomaly, whereas when the Gulf Stream is south of its mean position the profile has a negative anomaly. When the Gulf Stream is near its mean position, smaller anomalies of both signs are apparent.

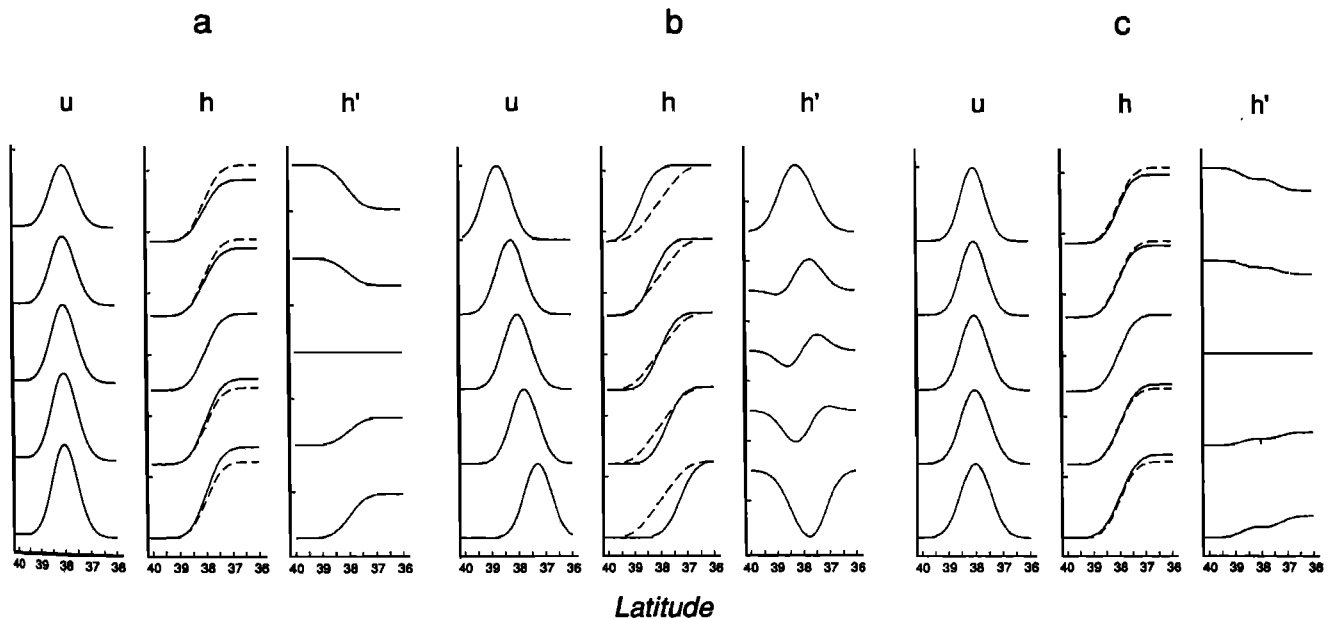


Fig. 2. Effects of varying the Gulf Stream model parameters. (a) Variations in amplitude  $a_1$  for (left) velocity profiles  $u$ , (center) height profiles  $h$ , obtained by integrating the velocity, and (right) height residuals  $h'$ , obtained by subtracting the mean height profile (center, dashed line). Height residuals are scaled up by a factor of 2, relative to the height. (b) same as Figure 2a, except for variations in position  $a_2$ . (c) same as Figure 2a except for variations in width  $a_3$ .

### 3. PROCESSING THE GEOSAT DATA

Collinear height profiles for three parallel subtracks crossing over the Gulf Stream (Plate 1), a total of 54 cycles from November 1986 through April 1989, were processed to obtain a series of residual sea surface heights. Raw altimeter heights were adjusted for tides, water vapor, tropospheric and ionospheric delays, and surface pressure using correction factors provided on the National Oceanographic Data Center (NODC) distribution tapes [Cheney *et al.*, 1987]. For each of the three subtracks studied, all of the cycles were interpolated to a common latitude-longitude grid with points separated by the sampling distance along the subtracks, 7.3 km. Parabolic orbit errors over  $30^\circ$  arcs were removed using a least squares fit of each profile to the mean profile for the subtrack, weighted by the inverse of the height variance. The temporal average profile, the geoid plus the mean Gulf Stream height, was removed from each height profile to produce residual heights.

Because the velocity profiles, which are proportional to the derivative of the height profiles, were needed to estimate the Gulf Stream parameters, the residual height profiles were filtered to remove instrument noise. Small gaps in the data were filled by linear interpolation, and the residual height profiles were low-pass filtered. The appropriate filter was determined from a comparison of velocity profiles from ADCP and Geosat along the subtrack from Bermuda to Cape Cod [Joyce *et al.*, 1990]. The choice of the filter was critical for the analysis of the Geosat data to obtain reasonable values for the maximum velocity  $a_1$  and the width  $a_3$  of the Gulf Stream; peak velocities from both Geosat and the ADCP exceeded  $2 \text{ m s}^{-1}$  after filtering. The height difference across the Gulf Stream was relatively insensitive to the choice of filter. We selected the filter which maximized the covariance between the Geosat data and the ADCP measurements 4 days earlier. The half-power point for this filter was 76 km.

### 4. OBTAINING THE MODEL PARAMETERS

Estimates of the parameters  $a_2$  and  $a_3$  from the residual heights and an initial guess for  $a_1$  were used to generate a series of height and velocity profiles based on (1) and (2). More precise parameter values for each time were obtained by fitting synthetic height profiles to the data with a simple least squares method. A flow chart for the entire procedure is shown in Figure 3.

#### Initial Estimates of the Parameters

Assuming that the Gulf Stream meanders to produce a mean velocity profile with a characteristic width much larger than its instantaneous width and a velocity maximum much smaller than its instantaneous value, the residual velocity should have a local maximum near the center of the Gulf Stream. If the Gulf Stream is near its mean position, however, the velocity maximum corresponding to the Gulf Stream may not be the largest value along the subtrack. The position and width parameters,  $a_2$  and  $a_3$ , were initially estimated from the residual geostrophic velocity  $u'$  (Figure 4b), which was computed from the residual height profile  $h'$  (Figure 4a), according to

$$u' = \frac{-g}{f} \frac{\partial h'}{\partial y} \quad (6)$$

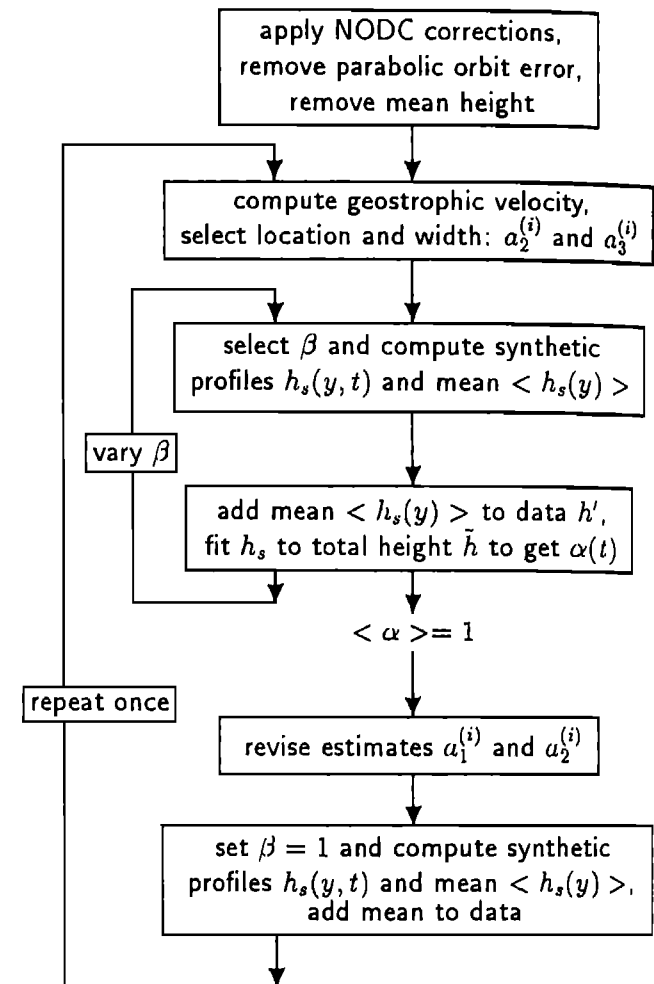


Fig. 3. Flow chart for the computation of the model parameters and the synthetic mean height profile. Two passes of the estimation and least squares fit were required to refine the parameter estimates.

A simple first difference was used to approximate the derivative. Typically, two or three possible velocity maxima (spaced 100 km or more apart) were identified for each cycle, but only one or two points fell within the possible range of the Gulf Stream meanderings. For cycle 12 (Figure 4b), there were local maxima (triangles) at about  $38^\circ\text{N}$  and  $35.5^\circ\text{N}$ . For about 80% of the cycles the appropriate choice for  $a_2$  was obvious from the magnitude and position of the velocity maximum. In the remaining cases a comparison with the previous or subsequent cycles suggested a best choice; in Figure 4 the northernmost maximum was selected because the average value for  $a_2$  from the other cycles was about  $38^\circ\text{N}$  and because the height and velocity profiles near  $35.5^\circ\text{N}$  had the characteristic signature of a cold-core ring. In one case the initial choice for  $a_2$  was subsequently rejected in favor of another position. For all of the subtracks the initial estimate for  $a_2$  varied between  $36^\circ$  and  $39^\circ\text{N}$ .

The full-width half-maximum  $L_{HM}$  was estimated from the positions where the residual velocity dropped to 30% of the local maximum value (circles in Figure 4). This criterion was selected empirically by comparing different initial width

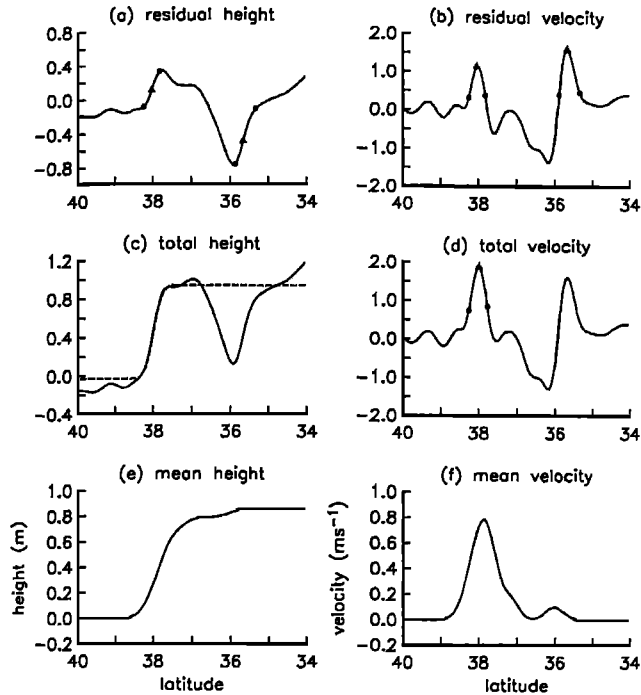


Fig. 4. Sea surface height and geostrophic velocity profiles. (a) Residual sea surface height and (b) corresponding geostrophic velocity. The initial estimate for  $a_2$  is indicated by the triangles and the estimate for  $a_3$  by the circles. (c) Estimated total height and (d) total geostrophic velocity. Revised estimates for  $a_2$  and  $a_3$  are indicated by the triangle and circles, respectively. (e) Mean sea surface height and (f) mean geostrophic velocity from the synthetic height profiles.

estimates with the final width needed to match the synthetic height profiles with the Geosat data. The value for  $L_{HM}$  was converted to an estimate of the parameter  $a_3$  using the formula

$$a_3 = \frac{L_{HM}}{2(2 \ln 2)^{1/2}} \quad (7)$$

#### Comparisons With AVHRR Data

To confirm the position of the Gulf Stream, residual heights were superimposed over the available Gulf Stream infrared (IR) images from the advanced very high resolution radiometer (AVHRR). In cases where the IR images were cloud-free over a large region, one velocity maximum corresponded closely to the center of the Gulf Stream as determined by its temperature signature (Plate 1). However, in cases where the Geosat data indicated two or more possible Gulf Stream positions, major Gulf Stream features were frequently obscured in the IR images by cloud cover. In these cases the temperature front corresponding to the northernmost velocity maximum was most often visible, leading us to select the northernmost position for  $a_2$  in the Geosat data. The Geosat residuals with a synthetic mean reinserted gave a more accurate and reliable method, described in the next section, to locate the Gulf Stream than the IR images. However, the IR images were helpful in distinguishing rings from meanders, and the statistical position information from Gilman [1988] was used to select a reasonable range of positions for the Gulf Stream along each subtrack.

#### Least Squares Fit to the Data

After estimates were made for  $a_2$  and  $a_3$ , which determine the shape of the height profile, the next step was to estimate  $a_1$ , which then determines the amplitude of the height difference across the Gulf Stream. To fit the synthetic height profiles to the residual height profiles from Geosat for each cycle, a rough estimate of the mean height profile was needed. We made four successive estimates of  $a_1(t)$  for each cycle and averaged the profiles to get four estimated mean height profiles. In the absence of any information about the temporal fluctuations of  $a_1$ , we set the first estimate of the maximum velocity to a constant,  $a_1^{(1)} = \beta$ . The estimated parameters  $a_2$  and  $a_3$  for each cycle, along with the initial guess for  $a_1$ , were used to generate a series of synthetic height profiles  $h_s(y, t)$  by integrating the Gaussian velocity profile as in (2). All of the synthetic height profiles were then averaged to generate an estimated mean Gulf Stream height profile  $\langle h_s(y) \rangle$ . The estimate of the mean height was added to the Geosat height residuals  $h'(y, t)$  to produce estimated total height profiles  $\tilde{h}(x, t)$ , that is,

$$\tilde{h}(y, t) = h'(y, t) + \langle h_s(y) \rangle \quad (8)$$

The synthetic height profiles were then fit to the total height profiles using a simple least squares fit which minimized

$$\sum_y [\tilde{h}(y, t) + \gamma - \alpha h_s(y + \delta, t)]^2 \quad (9)$$

where  $\gamma$  is a constant offset to account for uncorrected orbit errors,  $\delta$  is a shift to allow for small errors in the estimated position  $a_2$ , and  $\alpha$  gives the time variation of  $a_1$  according to

$$a_1^{(2)}(t) = \alpha(t) a_1^{(1)}(t) \quad (10)$$

The least squares fit was performed on a  $2^\circ$  latitude region centered on the estimated Gulf Stream position for that cycle. The fit was performed by varying in turn each of the parameters in small increments about an initial value which was 0 for  $\gamma$  and  $\delta$  and 1 for  $\alpha$ . The least squares fit was repeated several times varying  $\beta$  around the initial guess until the average of the factors  $\langle \alpha(t) \rangle$  was  $1.000 \pm 0.005$ . This convergence criterion made the new average of the series of height residuals consistent with the mean used to generate the synthetic total height for the fit, that is,

$$\langle a_1^{(i+1)}(t) \rangle \approx \langle \alpha(t) \rangle \langle a_1^{(i)}(t) \rangle = \langle a_1^{(i)}(t) \rangle \quad (11)$$

The mechanism for the convergence is discussed in the next section.

After this initial fit to the data, a new estimate of the mean height profile was made which incorporated the temporal variations in  $a_1$ , using the values of  $a_1^{(2)}(t)$  computed from (10), the original width estimates  $a_3$ , and the revised position estimates  $a_2 - \delta$ . This estimate of the mean was added to the residual height profiles and the entire process was repeated, starting with new position and width estimates (Figure 3). New estimates were made for  $a_2$  and  $a_3$  because the addition of the mean Gulf Stream shifted the position of the velocity maximum by as much as  $0.4^\circ$  latitude and altered the width. On this second pass the estimate  $L_{HM}$  was determined by the points where the velocity dropped to 40% of the local maximum; again this criterion was chosen empirically. This second estimate for

position and width gave us the opportunity to verify the initial choice of velocity maximum or to change the position of the Gulf Stream for one case in which the initial guess was wrong. For example, on cycle 12 (Figure 4) we initially selected the smaller velocity maximum at about 38°N; when the geostrophic velocity was computed from the total height profile, this local maximum was then larger than the maximum at 35.5°N, suggesting that our initial guess was correct. However, on cycle 20 we initially selected a velocity maximum at 37.8°N; we subsequently changed the position to 35.9°N. In a few cases we also adjusted the width because the criterion discussed above gave estimates which were either unrealistically wide or narrow when the height profile was complicated.

On the second pass through the estimation procedure (Figure 3) the third estimate for the maximum velocity was computed as a constant times the previous estimate,

$$a_1^{(3)}(t) = \beta a_1^{(2)}(t) \quad (12)$$

The parameter  $\beta$  was initially set at 1 and was varied to meet the convergence criterion discussed above. After the second least squares fit, the final synthetic height profiles and the mean height and velocity profiles were computed (Figure 4e and 4f).

Four versions of the mean height profile were used in this process: one before and after each of the two least squares fits of the synthetic height profiles to the data. The velocity profiles corresponding to these height profiles are shown in Figure 5, with the first estimate shown by a long-dashed

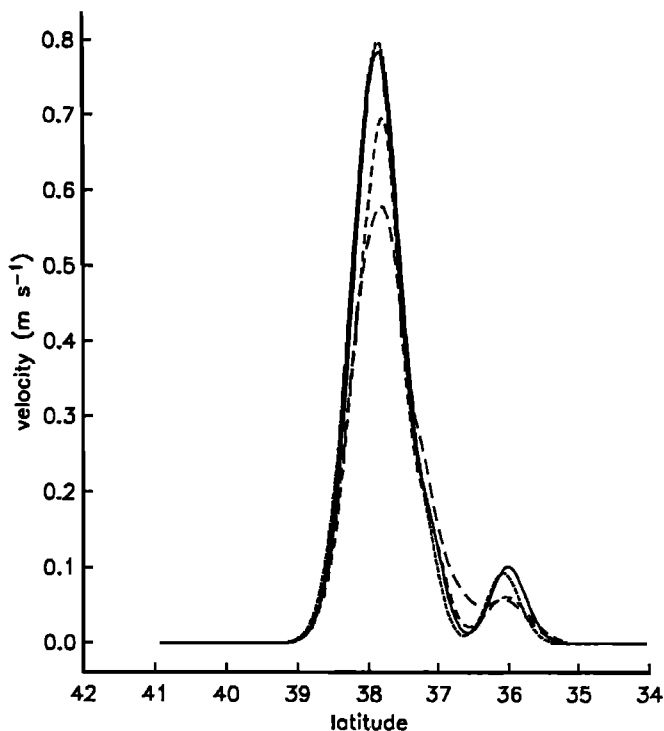


Fig. 5. Successive mean Gulf Stream geostrophic velocity profiles. The mean height profile was computed four times as the parameter estimates were refined; the center of the corresponding velocity profiles did not vary significantly from the initial guess (long-dashed line) to the final estimate (solid line). The secondary maximum in the velocity profile was due to the asymmetric distribution in Gulf Stream positions.

line and subsequent estimates corresponding to increasingly more solid lines. Because the Gulf Stream position could be determined unambiguously for most of the cycles, the position of the maximum in the mean varied only slightly in successive estimates. Between the first and second estimates the variations in  $a_1$  narrowed the mean jet and increased the primary velocity maximum from about 0.6 m s<sup>-1</sup> to about 0.7 m s<sup>-1</sup>. Between the second and third estimates the change in the Gulf Stream position for cycle 20 increased the secondary velocity maximum at about 36°N, while the revised width and the overall increase in amplitude of 5% further increased the peak mean velocity to nearly 0.8 m s<sup>-1</sup>. The fourth version of the mean differed only slightly from the third version.

### Convergence

A critical issue in evaluating the time series of parameters and the estimate of the mean height is the convergence of the iterative least squares fit procedure. To what are the iterations converging, and what factors determine the accuracy of the final result? The least squares fit essentially required the estimated total height to match a constant times the synthetic height, that is,

$$\tilde{h}(y, t) \approx \alpha(t) h_s(y, t) \quad (13)$$

where  $\tilde{h}(y, t)$  is given by (8). The estimated mean was obtained by averaging over the synthetic heights from all the cycles,

$$\langle h_s(y) \rangle = \langle a_1^{(i)} f(y) \rangle \quad (14)$$

where  $f(y, t)$  is the integral of the Gaussian velocity profile with the current estimates for  $a_2(t)$  and  $a_3(t)$ , and  $a_1^{(i)}(t)$  is the current estimate of  $a_1(t)$ . Using the Gaussian model to approximate the actual total height as  $a_1(t)f(t)$ , the estimate of the total height is the sum of the actual height residual and the synthetic mean so that

$$\tilde{h}(t) \approx a_1(t)f(t) - \langle a_1 f \rangle + \langle h_s(y) \rangle \quad (15)$$

where the  $y$  dependence is assumed. Neglecting correlations between  $a_1$  and the other parameters in  $f$  and using (14),

$$\begin{aligned} \tilde{h}(t) &\approx a_1(t)f(t) - \langle a_1 \rangle \langle f \rangle + \langle a_1^{(i)} \rangle \langle f \rangle \\ &\approx a_1(t)f(t) + \epsilon \langle f \rangle \end{aligned} \quad (16)$$

where  $\epsilon = \langle a_1^{(i)} \rangle - \langle a_1 \rangle$ , the mean error in the estimates. Combining (13), (14), and (16), the ratio of the estimated total height  $\tilde{h}(t)$  to the synthetic height  $h_s(y)$  is given by

$$\alpha = \frac{a_1(t)f(t) + \epsilon \langle f \rangle}{\langle a_1^{(i)} \rangle \langle f \rangle} \quad (17)$$

Now because the Gulf Stream meanders, the width over which the mean height rises is significantly larger than the instantaneous width, so that the error in mean height,  $\epsilon \langle f \rangle$  is comparable, in a least squares fit over a finite region, to an instantaneous profile of smaller amplitude,  $\epsilon' f(t)$ , as is shown in Figure 6, where  $|\epsilon'| < |\epsilon|$ . Thus

$$\alpha \approx \frac{a_1(t)f(t) + \epsilon' f(t)}{\langle a_1^{(i)} \rangle \langle f \rangle} \approx \frac{a_1(t) + \epsilon'}{\langle a_1^{(i)} \rangle} \quad (18)$$

which for small errors in the mean amplitude reduces to

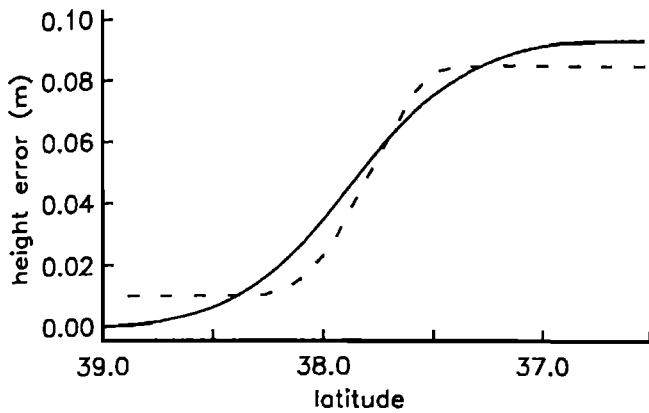


Fig. 6. The best least squares fit of an individual height profile to the error in the mean profile. The iterative fitting procedure converged because errors in the mean height profile (solid line) were approximated by incremental amplitudes in the individual height profiles (dashed line) smaller than the amplitude of the error in the mean. In the case illustrated here, the individual height profile has a center position which coincides with that of the mean height profile.

$$\alpha \approx \frac{a_1(t) + \epsilon' - \epsilon}{\langle a_1 \rangle} \quad (19)$$

Averaging  $\alpha$  over all the cycles gives

$$\langle \alpha \rangle = 1 + \frac{\epsilon' - \epsilon}{\langle a_1 \rangle} \quad (20)$$

so that for an estimate of the mean which is too large,  $\langle \alpha \rangle$  is less than 1 and for an estimate of the mean which is too small,  $\langle \alpha \rangle$  is greater than 1. When  $\langle \alpha \rangle = 1$ , then  $\langle a_1^{(t)} \rangle = \langle a_1 \rangle$ , that is, the mean of the estimates of  $a_1(t)$  is correct. The iterative fit will not converge when there is no significant difference between the scale width of the mean and that of the individual height profiles, that is, when the Gulf Stream does not meander a distance comparable to its width. Because the least squares fit depends on the difference in widths between an individual height profile and the mean profile, we did not adjust the width in the process of fitting the other parameters.

For this problem the first fit was performed for several estimates of  $\beta$  from 1.2 to 1.8  $\text{m s}^{-1}$  (Figure 7). The corresponding values for the average of the amplitude factors  $\langle \alpha \rangle$  fell nearly along a line, making the selection of the best estimate of  $\beta$  straightforward. For this subtrack the value of  $\beta$  for which the fit converged was 1.40 on the first pass and 1.05 on the second.

*The Crossing Angle*

To compute the cross-stream parameters  $u_d$  and  $w$ , the crossing angle  $\theta$  was estimated for 25 of the first 32 subtracks in the series (from November 1986 through April 1988) by comparing the position of the Gulf Stream on three adjacent subtracks. Estimates for the subtracks on either side were based on the initial estimates of  $a_2$  from the local maximum velocity. For each Geosat cycle an approximation to the Gulf Stream path was determined by fitting a cubic spline to the Gulf Stream positions  $a_2$  found for each of the three parallel subtracks (Figure 8) [Press, 1986]. The angle  $\theta$  between the subtrack and the line perpendicular to the spline was

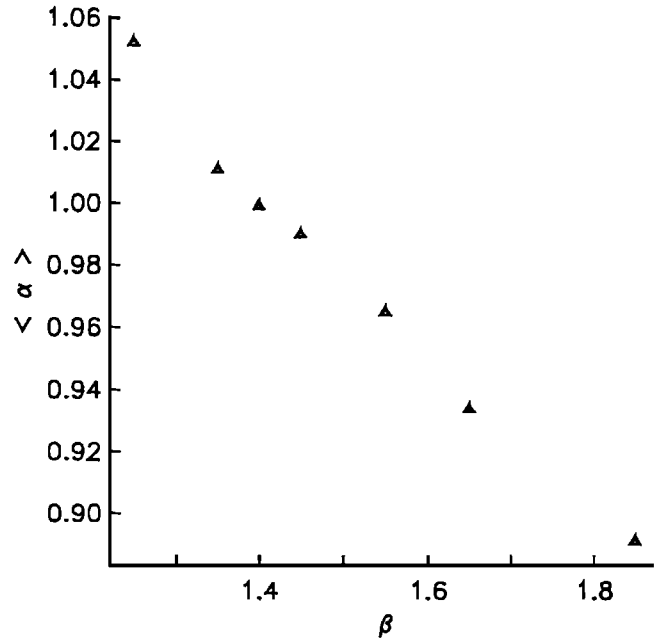


Fig. 7. Convergence criterion for the least squares fit. Synthetic height profiles and a mean profile were constructed using current parameter estimates and an amplitude factor,  $\beta$ . The best fit of the synthetic profiles to the total height profiles was computed for several values of  $\beta$ . The value of  $\beta$  (here 1.40) selected was that for which the temporal average of the factors  $\langle \alpha(t) \rangle$  was  $1.000 \pm 0.005$ .

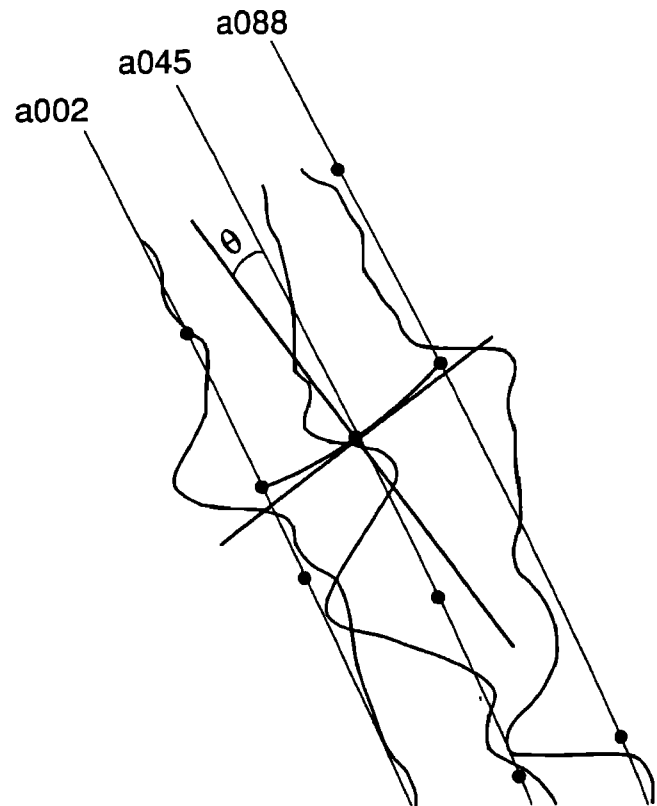


Fig. 8. Spline fit to the three maximum slopes corresponding to the Gulf Stream position. The angle between the perpendicular to the spline curve and the Geosat track determined the crossing angle  $\theta$ .

computed according to the formula

$$\cos \theta = \frac{\lambda_1 \lambda_2 + 1}{[(\lambda_1^2 + 1)(\lambda_2^2 + 1)]^{1/2}} \quad (21)$$

where  $\lambda_1$  and  $\lambda_2$  are the slopes of the subtrack and the perpendicular to the spline fit, respectively.

## 5. RESULTS

### The Synthetic Profiles

Synthetic and estimated total height profiles agreed closely in the vicinity of the Gulf Stream, although significant departures were apparent due to rings (for example, cycles 13 and 52, Figure 9). On at least one occasion (cycle 20) there was a triple crossing of the Gulf Stream, resulting in two possible positions; we chose to model the crossing with the largest height difference. For three cycles (7, 20, and 22) the Gulf Stream was significantly south of its mean position; available IR images showed that these southward excursions corresponded to meanders of the Gulf Stream. The height anomalies associated with the rings and the southward excursions dominated the variability of the height residuals because the mean height was removed.

### Parameter Values

The values of the alongtrack parameters  $a_1$ ,  $a_2$ , and  $a_3$  for each cycle are shown in Table 1, the cross-stream parameters are shown in Table 2, and the statistics for all parameters

are shown in Table 3. Values for the width are given in kilometers; the corresponding distance in terms of alongtrack latitude can be computed given the local angle between the subtrack and lines of constant latitude, which is  $67^\circ$  at  $38^\circ\text{N}$ . This yields approximately 121 km per degree of alongtrack latitude.

The relative fluctuations in the position  $a_2$  of the Gulf Stream were large compared with the other parameters, so that the ratio of fluctuations in position to average scale width,  $\sigma_2 / \langle a_3 \rangle$ , was 2.5, where  $\sigma_2$  is the standard deviation of  $a_2$ . Based on the root-mean-square (rms) magnitude of  $\delta$  in (9), the least squares fit, the estimated error for each individual measurement of  $a_2$  was  $\pm 9.2$  km (or  $0.076^\circ$  latitude) along the subtrack. This corresponds to an estimated error in the mean position,  $\langle a_2 \rangle$ , of about 1.3 km ( $0.011^\circ$  latitude.)

The mean alongtrack width parameter  $a_3$  was 24.1 km, with a standard deviation of 5.6 km. The relative size of fluctuations in the width parameter was small, with the ratio  $\sigma_3 / \langle a_3 \rangle$  about 0.23. The errors in width were small, probably less than 5%, for most of the cycles; the only large errors occurred where the height profile was complicated, as in cycles 34, 43, and 47 (Figure 9). In these cases the Geosat subtrack probably crossed the Gulf Stream near a meander.

The mean value of the maximum velocity  $a_1$  was  $1.48 \text{ m s}^{-1}$  and the standard deviation was 0.34, for a standard-deviation-to-mean ratio of 0.23. It is difficult to

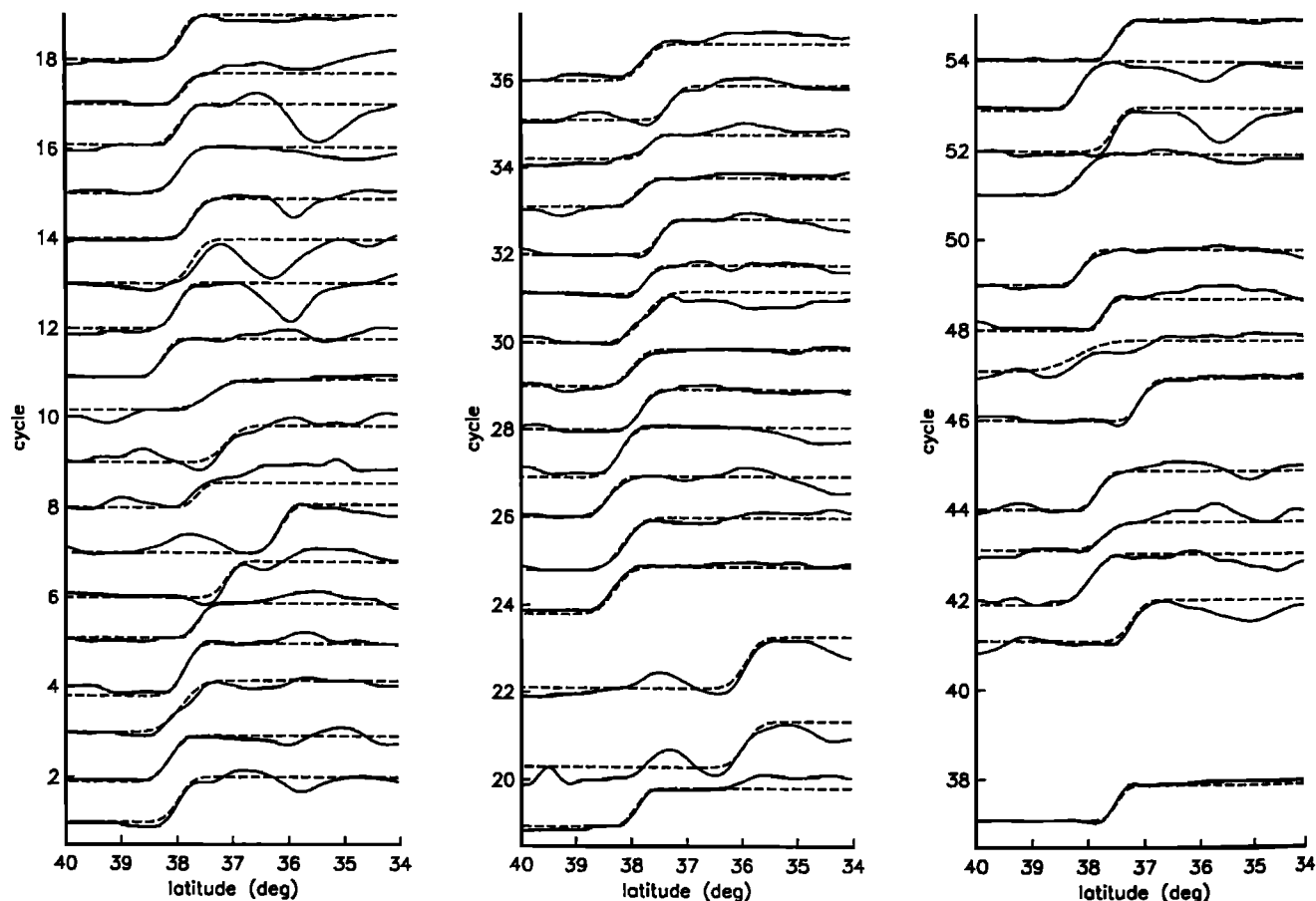


Fig. 9. Estimated total height and synthetic height profiles for subtrack a045. Low-pass-filtered sea surface height plus the synthetic mean height (solid lines) and synthetic height (dashed

lines) generated from estimates of  $a_1$ ,  $a_2$  and  $a_3$  after the final least squares fit. Cycles (left) 1-18, (center) 19-36, and (right) 37-54, offset by 1 m.

TABLE 1. Gulf Stream Model Parameters for Ascending Subtrack 45

| Cycle | Year | Day | $a_1$ ,<br>$\text{m s}^{-1}$ | $a_2$<br>$^{\circ}\text{N}$ | $a_3$ ,<br>$\text{km}$ | $U$ ,<br>$10^5 \text{m}^2 \text{s}^{-1}$ |
|-------|------|-----|------------------------------|-----------------------------|------------------------|--|
| 1     | 1986 | 315 | 1.74                         | 37.98                       | 22.9                   | 1.075                                    |
| 2     | 1986 | 332 | 1.56                         | 38.14                       | 25.4                   | 1.072                                    |
| 3     | 1986 | 349 | 1.18                         | 37.98                       | 33.1                   | 1.055                                    |
| 4     | 1987 | 001 | 2.00                         | 37.87                       | 22.9                   | 1.236                                    |
| 5     | 1987 | 018 | 1.68                         | 37.61                       | 17.8                   | 0.809                                    |
| 6     | 1987 | 035 | 1.49                         | 37.12                       | 20.4                   | 0.820                                    |
| 7     | 1987 | 052 | 1.86                         | 36.15                       | 22.9                   | 1.155                                    |
| 8     | 1987 | 069 | 0.94                         | 37.66                       | 23.6                   | 0.601                                    |
| 9     | 1987 | 086 | 1.09                         | 37.07                       | 28.3                   | 0.834                                    |
| 10    | 1987 | 103 | 0.71                         | 37.39                       | 38.2                   | 0.733                                    |
| 11    | 1987 | 120 | 1.68                         | 38.25                       | 20.3                   | 0.924                                    |
| 12    | 1987 | 137 | 1.93                         | 37.98                       | 20.3                   | 1.058                                    |
| 13    | 1987 | 154 | 1.50                         | 37.71                       | 22.9                   | 0.927                                    |
| 14    | 1987 | 171 | 1.70                         | 37.71                       | 20.3                   | 0.934                                    |
| 15    | 1987 | 188 | 1.60                         | 37.93                       | 25.4                   | 1.102                                    |
| 16    | 1987 | 205 | 1.56                         | 37.87                       | 22.9                   | 0.964                                    |
| 17    | 1987 | 222 | 1.33                         | 37.82                       | 20.3                   | 0.730                                    |
| 18    | 1987 | 239 | 1.91                         | 37.87                       | 20.3                   | 1.047                                    |
| 19    | 1987 | 256 | 1.70                         | 37.93                       | 20.3                   | 0.931                                    |
| 20    | 1987 | 273 | 1.53                         | 35.93                       | 25.5                   | 1.058                                    |
| 21    | 1987 | 290 |                              |                             |                        |  |
| 22    | 1987 | 307 | 1.76                         | 35.93                       | 25.5                   | 1.216                                    |
| 23    | 1987 | 326 |                              |                             |                        |  |
| 24    | 1987 | 341 | 1.52                         | 38.30                       | 27.9                   | 1.148                                    |
| 25    | 1987 | 358 | 1.53                         | 38.09                       | 30.5                   | 1.261                                    |
| 26    | 1988 | 010 | 1.44                         | 38.41                       | 25.4                   | 0.989                                    |
| 27    | 1988 | 027 | 1.82                         | 38.20                       | 25.4                   | 1.246                                    |
| 28    | 1988 | 044 | 1.78                         | 37.82                       | 20.3                   | 0.977                                    |
| 29    | 1988 | 061 | 1.34                         | 37.98                       | 25.4                   | 0.920                                    |
| 30    | 1988 | 078 | 1.20                         | 37.82                       | 33.1                   | 1.071                                    |
| 31    | 1988 | 095 | 1.39                         | 37.72                       | 17.8                   | 0.670                                    |
| 32    | 1988 | 112 | 1.54                         | 37.50                       | 20.4                   | 0.848                                    |
| 33    | 1988 | 129 | 1.08                         | 37.87                       | 22.9                   | 0.671                                    |
| 34    | 1988 | 146 | 0.78                         | 37.88                       | 23.6                   | 0.498                                    |
| 35    | 1988 | 163 | 1.36                         | 37.28                       | 20.4                   | 0.746                                    |
| 36    | 1988 | 180 | 1.28                         | 37.77                       | 25.4                   | 0.878                                    |
| 37    | 1988 | 197 | 1.71                         | 37.50                       | 17.8                   | 0.824                                    |
| 38    | 1988 | 214 |                              |                             |                        |  |
| 39    | 1988 | 231 |                              |                             |                        |  |
| 40    | 1988 | 249 |                              |                             |                        |  |
| 41    | 1988 | 266 | 1.62                         | 37.23                       | 22.9                   | 1.003                                    |
| 42    | 1988 | 283 | 1.47                         | 37.98                       | 30.5                   | 1.211                                    |
| 43    | 1988 | 300 | 0.87                         | 37.71                       | 28.3                   | 0.667                                    |
| 44    | 1988 | 317 | 1.71                         | 37.82                       | 20.3                   | 0.942                                    |
| 45    | 1988 | 334 |                              |                             |                        |  |
| 46    | 1988 | 351 | 1.78                         | 37.07                       | 20.4                   | 0.979                                    |
| 47    | 1989 | 002 | 0.43                         | 38.11                       | 47.2                   | 0.545                                    |
| 48    | 1989 | 019 | 1.78                         | 37.71                       | 15.3                   | 0.735                                    |
| 49    | 1989 | 036 | 1.52                         | 38.14                       | 20.3                   | 0.833                                    |
| 50    | 1989 | 053 |                              |                             |                        |  |
| 51    | 1989 | 070 | 1.21                         | 38.14                       | 30.5                   | 0.998                                    |
| 52    | 1989 | 087 | 1.88                         | 37.55                       | 20.4                   | 1.032                                    |
| 53    | 1989 | 104 | 1.69                         | 38.14                       | 25.4                   | 1.160                                    |
| 54    | 1989 | 121 | 1.59                         | 37.50                       | 22.9                   | 0.983                                    |

TABLE 2. Model Parameters Corrected for Crossing Angle

| Cycle | $\cos \theta$ | $w$ ,<br>$\text{km}$ | $u_d$<br>$\text{m s}^{-1}$ |
|-------|---------------|----------------------|----------------------------|
| 2     | 0.984         | 25.0                 | 1.59                       |
| 3     | 0.990         | 32.8                 | 1.19                       |
| 4     | 0.981         | 22.5                 | 2.04                       |
| 5     | 0.845         | 15.0                 | 1.99                       |
| 6     | 0.864         | 17.6                 | 1.72                       |
| 7     | 0.871         | 20.0                 | 2.14                       |
| 8     | 0.655         | 15.5                 | 1.44                       |
| 9     | 0.890         | 25.2                 | 1.22                       |
| 10    | 0.922         | 35.2                 | 0.77                       |
| 11    | 0.841         | 17.1                 | 2.00                       |
| 12    | 0.974         | 19.8                 | 1.98                       |
| 13    | 0.978         | 22.4                 | 1.53                       |
| 14    | 0.992         | 20.1                 | 1.71                       |
| 15    | 0.998         | 25.5                 | 1.60                       |
| 16    | 0.992         | 22.7                 | 1.57                       |
| 18    | 0.965         | 19.6                 | 1.98                       |
| 19    | 0.968         | 19.7                 | 1.76                       |
| 24    | 0.745         | 20.8                 | 2.04                       |
| 25    | 0.976         | 29.8                 | 1.57                       |
| 26    | 0.930         | 23.6                 | 1.55                       |
| 27    | 0.978         | 24.8                 | 1.86                       |
| 28    | 0.966         | 19.6                 | 1.84                       |
| 30    | 1.000         | 33.1                 | 1.20                       |
| 31    | 0.976         | 17.4                 | 1.42                       |
| 32    | 0.940         | 19.2                 | 1.64                       |

quantify the errors in the maximum velocity  $a_1$ , since these values were derived from the least squares fit and depend on the accuracy of the other parameters, the convergence of the iterative fitting procedure, and on the appropriateness of the Gaussian model. However, in a comparison of Geosat with ADCP velocities along subtrack a088, the rms difference between a Geosat profile and an ADCP cross-track velocity profile taken 4 days earlier was only  $0.23 \text{ m s}^{-1}$ . Considerable changes in the Gulf Stream were apparent in ADCP profiles separated by a week, suggesting that much of this difference was due to temporal variability, not errors in the Geosat velocity. The difference in the profiles was not noticeably larger in the vicinity of the peak contribution of the synthetic mean current.

The surface transport,  $U$ , given by

$$\begin{aligned}
 U &= \int_{-\infty}^{\infty} u(y) dy \\
 &= (2\pi)^{1/2} a_1 a_3 \quad (22)
 \end{aligned}$$

had a mean value of  $0.94 \times 10^5 \text{ m}^2 \text{ s}^{-1}$  and a standard deviation of  $0.19 \times 10^5 \text{ m}^2 \text{ s}^{-1}$ . Because the least squares fitting procedure minimized the height differences for a fixed width estimate, the best estimate of the transport error comes from the misfit to the height profiles. The rms fraction of the height variance which could not be accounted for by the synthetic height profiles according to (9) was 0.010. For a typical  $\Delta h$  of 1 m, the height variance is about  $0.25 \text{ m}^2$ , for

TABLE 3. Statistics of Parameters

| Parameter                            | Mean<br>< $a$ > | Standard<br>Deviation<br>$\sigma$ | Ratio<br>$\sigma / \langle a \rangle$ |
|--------------------------------------|-----------------|-----------------------------------|---------------------------------------|
| $a_1, \text{ms}^{-1}$                | 1.48            | 0.34                              | 0.23                                  |
| $a_2, ^\circ\text{N}$                | 37.68           | 0.55                              | 2.5*                                  |
| $a_3, \text{km}$                     | 24.1            | 5.6                               | 0.23                                  |
| $U, 10^5 \text{ m}^2 \text{ s}^{-1}$ | 0.94            | 0.19                              | 0.20                                  |
| $\cos \theta^\dagger$                | 0.93            | 0.084                             | 0.09                                  |
| $w, \dagger \text{ km}$              | 22.6            | 5.4                               | 0.24                                  |
| $u_d, \dagger \text{ m s}^{-1}$      | 1.65            | 0.33                              | 0.20                                  |

\*Ratio of position fluctuation to mean width,  $\sigma_2 / \langle a_3 \rangle$ .

†Statistics for  $\cos \theta$ ,  $w$ , and  $u_d$  are for the first 32 cycles only.

an rms height error of 0.050 m, which in turn corresponds to a transport error of  $0.046 \times 10^5 \text{ m}^2 \text{ s}^{-1}$ .

The mean of the cosine of the crossing angle  $\langle \cos \theta \rangle$ , for the 25 cycles for which all three subtracks had good data available, was 0.93 with a standard deviation of 0.08. Most of the time the subtrack crossed the Gulf Stream at an angle greater than  $58^\circ$ . The estimated error for each individual measurement was about 0.05, which is nearly as large as the standard deviation.

The actual width parameter  $w$  from (3) had a mean value of about 25 km, which corresponds to a value of  $L_{HM}$  of 60 km, and a standard deviation of 5.8 km. The ratio of standard deviation to mean was comparable to that for  $a_3$ , suggesting again that it was not dominated by the errors in  $\cos \theta$ . The maximum downstream velocity, which was derived from (4), had a mean value of  $1.65 \text{ m s}^{-1}$  and a standard deviation of  $0.33 \text{ m s}^{-1}$ .

#### Mean and Time Series of Parameters

The mean height profile, estimated from the synthetic height profiles, shows a 0.86-m rise centered on the mean Gulf Stream position, about  $37.7^\circ\text{N}$  (Figure 4e). The maximum velocity of the mean Gulf Stream was about  $0.79 \text{ m s}^{-1}$ ; a secondary maximum of about  $0.09 \text{ m s}^{-1}$  occurred at about  $36^\circ\text{N}$  (Figure 4f). The three cycles with large southward excursions caused the secondary maximum; in fact the shape of the mean current is primarily a function of the position statistics which can be seen by examining the histogram (Figure 10). The asymmetry in the structure of the mean Gulf Stream surface current is due to the asymmetry in the position statistics because only symmetric Gaussian velocity profiles were used to construct it.

The time series of the model parameters and the surface transport (Figure 11) show some correlations between the parameters. The maximum velocity  $a_1$  was at a minimum in the spring of both 1987 and 1988, although low values were also attained in the winter of 1988–1989. The fluctuations in alongtrack width  $a_3$  were dominated by a large width increase between October 1987 and March 1988. Surface transport, which is the product of these two variables, had low values in the spring and high values in the late fall, corresponding to the minima in the maximum velocity. Surface transport is primarily a function of peak velocity

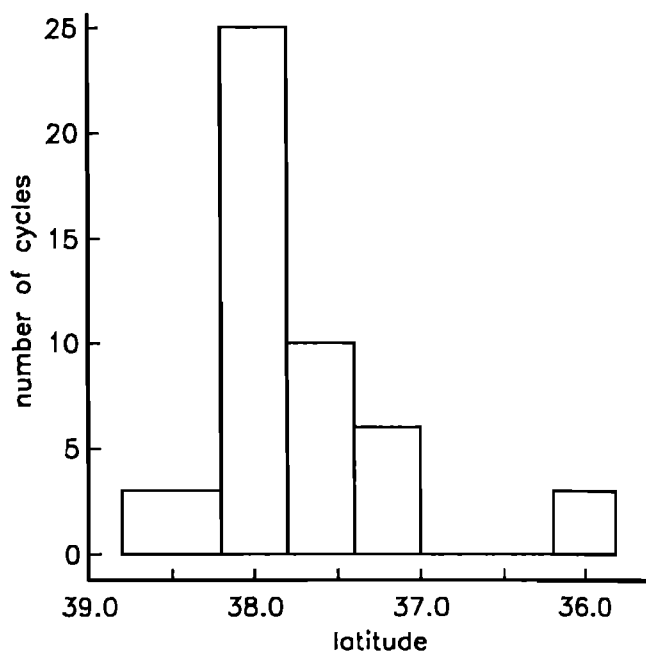


Fig. 10. Histogram of Gulf Stream center positions. The asymmetry in the distribution of center positions  $a_2$  around the mean position at  $37.7^\circ\text{N}$  was responsible for the asymmetry in the mean Gulf Stream velocity profile, which was constructed from symmetric Gaussian profiles. The three cycles centered near  $36^\circ\text{N}$  caused the secondary velocity maximum (see Figure 5).

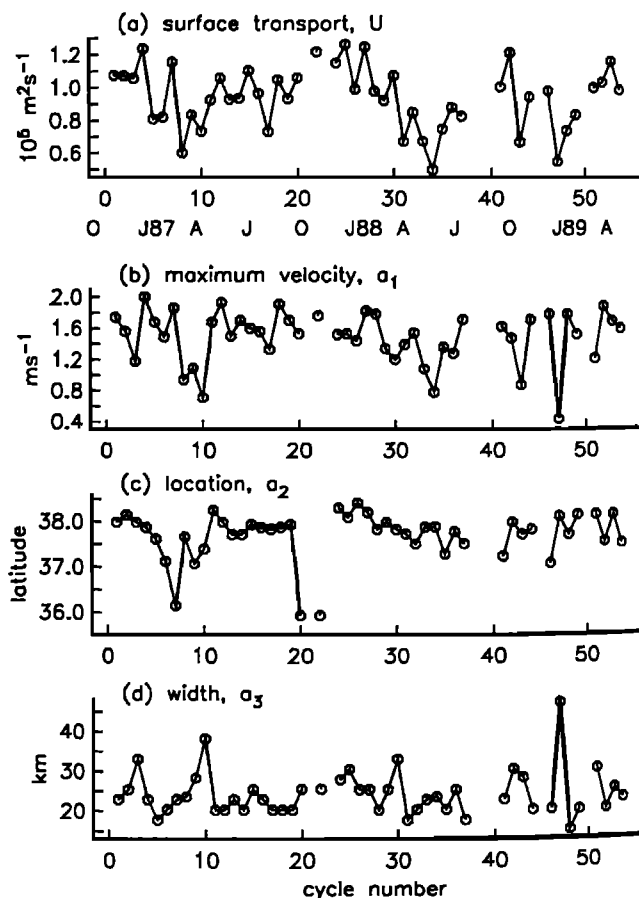


Fig. 11. Time series of alongtrack model parameters and surface transport. (a) The integrated surface transport  $U$ , (b) the Gulf Stream maximum velocity  $a_1$ , (c) the center position  $a_2$ , and (d) the width parameter  $a_3$ . Center positions near  $36^\circ\text{N}$  correspond to large meanders of the Gulf Stream.

$a_1$  with a correlation coefficient ( $r^2$ ) of 0.84, although it is sometimes modified by the width, as in the fall and winter of 1987–1988. Maximum surface transport was about twice the magnitude of the minimum transport. Maximum transport occurred when the Gulf Stream was north of its mean position, with a transport minimum when it was south of its mean position. The exceptions to this pattern were the fall and winter of 1988–1989 and the southward excursions of the Gulf Stream on cycles 20 and 22.

#### Cross-Stream Parameters

Time series of the estimated actual width  $w$  (perpendicular to the Gulf Stream axis) and the maximum downstream velocity  $u_d$  were for the most part, similar to the time series of alongtrack width and maximum cross-track velocity (compare Figure 11 and Figure 12). There do not appear to be spurious fluctuations in either velocity or width due to systematic deviations from a perpendicular crossing of the Gulf Stream. The increase in width between cycles 20 and 27 is reflected in the larger cross-stream widths for cycles 24 through 27. Fluctuations in the maximum velocities are also similar. Thus in general, the parameters computed without regard to crossing angle gave reasonable time series of fluctuations, although of course on average, the along-track width was larger than the cross-stream width and the cross-track velocity was smaller than the downstream velocity. Because of the difficulty in obtaining estimates of the crossing angle and the qualitative similarity of the cross-stream and alongtrack parameters for the first 32 cycles, we subsequently used changes in  $a_3$  and  $a_1$  to indicate changes in the actual velocity and width.

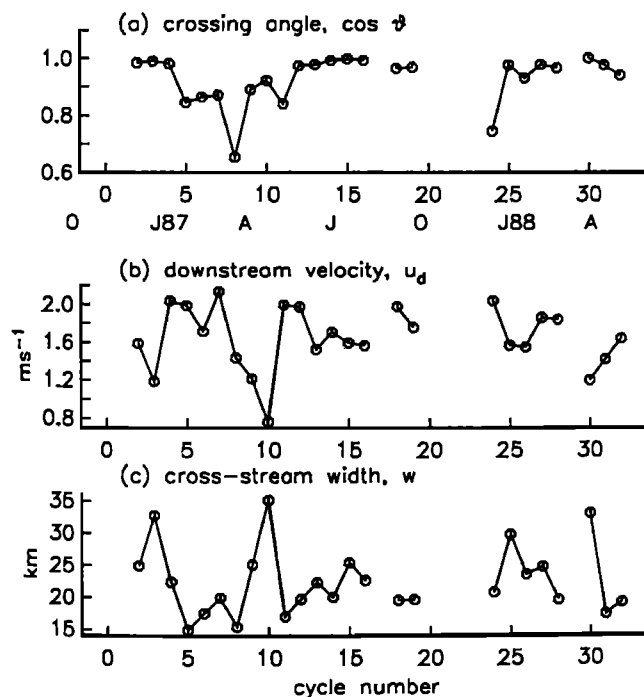


Fig. 12. Time series of cross-stream model parameters. (a) Crossing angle  $\theta$ , (b) maximum downstream velocity  $u_d$ , and (c) width  $w$  computed using the crossing angle estimate. The similarity between these parameters and the corresponding parameters in Figure 11 suggests that crossing angle variations were not primarily responsible for temporal fluctuations in the alongtrack parameters.

## 6. DISCUSSION

### The Synthetic Data Method

The individual Gulf Stream velocity profiles do not have to be Gaussian for this method to give a useful estimate of the mean height profile. The primary factors influencing the mean profile were the statistics of the Gulf Stream position, because of the large meanders, and the height difference across the jet, which is the integral of the velocity profile and is therefore not very sensitive to the details of its shape. Thus the mean obtained assuming a Gaussian velocity profile can be added to the residual height profiles to obtain estimated total height profiles, which may not resemble Gaussian jets. The primary disadvantage in using the Gaussian profile was not its shape but its failure to model large cold-core eddies or multiple crossings of the Gulf Stream. An advantage of using a parameterization of the profiles is that we reduced the description of the Gulf Stream kinematics to a few time series of parameters in the same simple operation that produced an estimate of the mean.

This method of obtaining parameter estimates is straightforward in concept and inexpensive in terms of computer time, although somewhat complex in practice. The step of generating synthetic profiles required the most computations: each set of synthetic profiles and mean (one for each value of  $\beta$ , Figure 3) required less than 6 min of CPU time on a Sun 3/50. Some of the procedures could be automated more than was done here; however, it is hard to eliminate some of the intermediate steps without getting inaccurate results. For example, for those few cycles with complicated profiles it was necessary to adjust the automatic estimates of width and position to get sensible results. Also, to distinguish between a ring and the Gulf Stream or between multiple crossings of the Gulf Stream, the estimated total height profiles were plotted before the final computation of the synthetic profiles.

No attempt was made here to determine the height field on larger scales. Thus this method, as currently implemented, does not describe the recirculation pattern of the Gulf Stream region. Nor does it describe the large-scale mean height field, which can more readily be obtained by subtracting the available large-scale geoid from the average large-scale height field following *Tai and Wunsch* [1984].

### Comparisons With Other Measurements

These results agree qualitatively with studies of the Gulf Stream north wall positions by *Gilman* [1988], which show that the mean position shifts further north and the standard deviation increases downstream. The quantitative agreement with the north wall position statistics, based on years 1982–1986, is excellent (Table 4). Note that variations in the mean and standard deviations of the north wall positions reflect interannual variability. The Geosat Gulf Stream position, which is a measure of the position of the center of the jet, is 36–48 km south (along the subtrack) of the mean north wall position for the region studied. The standard deviation from Geosat is within the variability of the north wall values at 68°W, somewhat higher at 69.4°W, where the north wall values are anomalously low, and a bit lower at 70.8°W. North wall statistics for the Geosat time period are not yet available.

The mean magnitude of the surface transport is consistent with estimates made by *Richardson* [1985] of the eastward

TABLE 4. Comparison of Geosat and AVHRR Gulf Stream Positions

| Geosat<br>Subtrack | Longitude,<br>°W | AVHRR*                  |             | Geosat                  |             |
|--------------------|------------------|-------------------------|-------------|-------------------------|-------------|
|                    |                  | Mean <sup>†</sup><br>°N | s.d.,<br>km | Mean <sup>†</sup><br>°N | s.d.,<br>km |
| a002               | 70.8             | 37.5–38.2               | 49–51       | 37.6                    | 37          |
| a045               | 69.4             | 38.0–38.2               | 49–51       | 37.7                    | 67          |
| a088               | 68.0             | 37.8–38.3               | 60–78       | 37.7                    | 70          |

\*AVHRR north wall locations for 1982–1986 from *Gilman* [1988].

<sup>†</sup>AVHRR data give the north wall location. Geosat gives the location of the center of the Gulf Stream. Range of values in AVHRR reflects interannual variability.

surface transport of the Gulf Stream at 55°W. The mean value from this analysis of  $0.94 \times 10^5 \text{ m}^2 \text{ s}^{-1}$  at 69°W compares favorably with Richardson's estimate of  $1.22 \times 10^5 \text{ m}^2 \text{ s}^{-1}$ , suggesting a 30% increase in surface flow downstream.

The maximum velocity estimates are consistently higher than the  $0.7 \text{ ms}^{-1}$  typically found by *Tai* [1990], who analyzed Geosat data for the Gulf Stream using the difference of Geosat velocity profiles; the favorable comparison of our peak velocities for subtrack a088 with ADCP measurements [*Joyce et al.*, 1990] suggests that *Tai's* filter, which had a

half-power point of approximately 215 km, removed much of the smaller-scale oceanic signal.

The annual signals for surface transport and position were calculated by averaging the available estimates (Figure 13). There were insufficient measurements to justify monthly resolution, so the values were binned into 2-month intervals for averaging. The average of all position estimates (Figure 13a, solid line) shows a dramatic southward shift in September–October, but this is primarily due to a single estimate near 36°N. Therefore we recomputed the positions excluding cycles 7, 20, and 22, for which the positions were clearly due to large meanders, to obtain the dashed line in Figure 13a. This latter curve shows an annual signal with more northerly positions in November–February and more southerly positions in March–October. This represents a considerable lag from the results of *Tracey and Watts* [1986], who observed the annual signal in the Gulf Stream position from inverted echo sounders; they found the more northerly positions in the summer–fall and more southerly positions in the winter–spring. However, they also noted significant interannual variability in the positions. The surface transport (Figure 13b) shows a minimum in May–June and a maximum in November–December, in marked contrast with the annual signal seen by *Fu et al.* [1987] which had a maximum transport in April and a minimum in December. The annual signal of *Fu et al.* was based on altimeter data from a larger region, from about 70° to 74°W; the transport fluctuations seen here for a single subtrack may be due to smaller-scale Gulf Stream variability. Other measurements of surface transport summarized by *Tracey and Watts* show two maxima and minima in the annual cycle, making direct comparisons difficult; however all show minimum transport in October. In particular *Fuglister* [1951] shows an annual cycle nearly the reverse of that in Figure 13b.

#### Future Analysis

The success of this method on one subtrack suggests that its extension to the entire Gulf Stream in a forthcoming paper will produce reliable time series of width, position, velocity, and surface transport about every 100 km along the Gulf Stream and an estimate of the mean sea surface topography relative to the geoid. An analysis of these time series will give a description of the local kinematics of the Gulf Stream, the spatial scales of variability, the fluctuations of surface transport as a function of downstream location, and possibly propagation of fluctuations along the Gulf Stream.

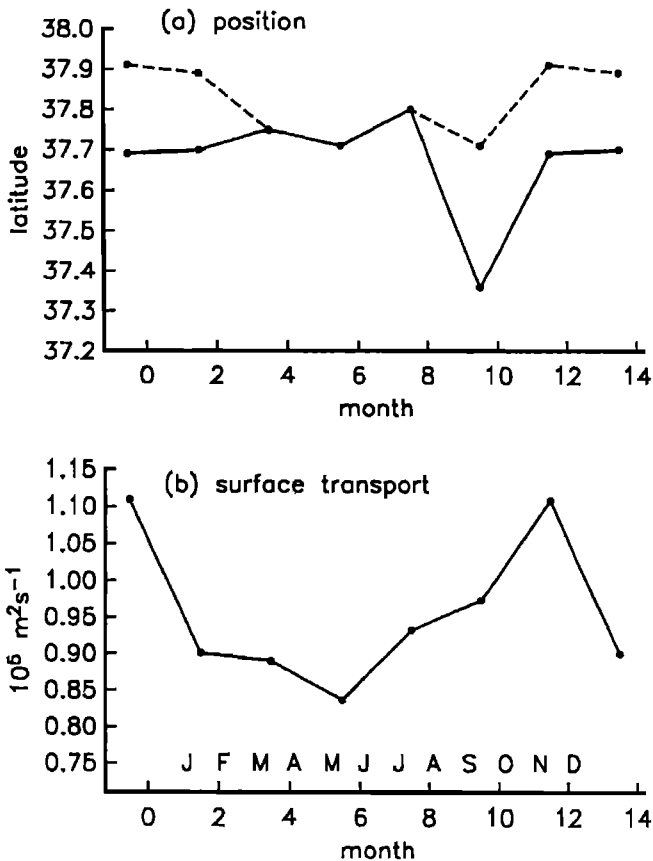


Fig. 13. The average annual cycles for (a) position and (b) surface transport. Values were binned into 2-month intervals and averaged over the 2.5-year series. Solid lines represent averages for all the data. The dashed line in Figure 13a is the average position with cycles 7, 20, and 22 removed. The first and last points are repeated for clarity.

## 7. CONCLUSIONS

A Gaussian velocity profile for the Gulf Stream was used to model sea surface height fluctuations for an ascending Geosat subtrack. Based on a comparison between the model and the data, estimates were made for the position and alongtrack width of the Gulf Stream; these estimates were used to generate synthetic sea surface height profiles and also an estimate of the mean alongtrack height relative to the geoid. The synthetic height profiles were iteratively fit to the data with a simple least squares procedure.

An analysis of the convergence of the iterative fitting procedure showed that for regions where the Gulf Stream meanders at least its width from its mean position, the estimate of the mean height should converge to the actual height.

Comparisons between position statistics from Geosat and AVHRR data were excellent, with the estimated center of the Gulf Stream approximately half the width of the Gulf Stream south of the north wall positions and showing comparable position variability.

The mean magnitude of the surface transport for the Gulf Stream estimated from this study at 69°W was approximately 30% smaller than an estimate made by Richardson [1985] at 55°W, consistent with a model of increasing transport in the downstream direction.

Time series of the maximum velocity, width, position, and surface transport suggested an annual cycle with a transport minimum in May–June and a maximum in November–December, in contrast with some previous results from altimetry and other surface transport measurements. The annual transport maximum (minimum) coincided with a northerly (southerly) position of the Gulf Stream.

*Acknowledgments.* T. Joyce suggested using the Gaussian model to estimate mean height profiles. The Geosat processing programs were written by M. Caruso, Z. Sirkes and P. Flament. The authors would like to thank P. Flament, D. Kelley, and S. Lentz for helpful discussions on the analysis and processing techniques and M. Caruso for assistance in processing of the data. S. Gille was a WHOI summer student fellow for most of the duration of this research. K. Kelly was supported by the Office of Naval Research on contract N00014-86-K-0751 (University Research Initiative). Woods Hole Oceanographic Institution contribution 6900.

## REFERENCES

Calman, J., Introduction to sea-surface topography from satellite altimetry, *Johns Hopkins APL Tech. Dig.*, 8, 206–211, 1987.

- Cheney, R. E., B. C. Douglas, R. W. Agreen, L. Miller, D. L. Porter, and N. S. Doyle, Geosat altimeter geophysical data record user handbook, *NOAA Tech. Memo. NOS NGS-46*, 29 pp., Natl. Ocean. Serv., Rockville, Md., 1987.
- Cornillon, P., The effect of the New England seamounts on Gulf Stream meandering as observed from satellite IR imagery, *J. Phys. Oceanogr.*, 16, 386–389, 1986.
- Fu, L.-L., J. Vazquez, and M. Parke, Seasonal variability of the Gulf Stream as observed from satellite altimetry, *J. Geophys. Res.*, 92, 749–754, 1987.
- Fuglister, F. C., Annual variations in current speeds in the Gulf Stream system, *J. Mar. Res.*, 10, 119–127, 1951.
- Gilman, C. S., A study of the Gulf Stream downstream of Cape Hatteras 1975–1986, M.S. thesis, Univ. of R.I., Kingston, RI, 75 pp., 1988.
- Hall, M. M., and H. L. Bryden, Profiling the Gulf Stream with a current meter mooring, *Geophys. Res. Lett.*, 12, 203–206, 1985.
- Joyce, T. M., C. Wunsch, and S. D. Pierce, Synoptic Gulf Stream velocity profiles through simultaneous inversion of hydrographic and acoustic Doppler data, *J. Geophys. Res.*, 91, 7573–7585, 1986.
- Joyce, T. M., K. A. Kelly, D. M. Schubert, and M. J. Caruso, Shipboard and altimetric studies of rapid Gulf Stream variability between Cape Cod and Bermuda, *Deep Sea Res.*, in press, 1990.
- Mitchell, J. M., Z. R. Hallock, and J. D. Thompson, REX and Geosat: progress in the first year, *Johns Hopkins APL Tech. Dig.*, 8, 234–244, 1987.
- Press, W. H., B. P. Flannery, S. A. Teukolsky, and W. T. Vetterling, *Numerical Recipes*, 818 pp., Cambridge University Press, New York, 1986.
- Richardson, P. L., Average velocity and transport of the Gulf Stream near 55°W, *J. Mar. Res.*, 43, 83–111, 1985.
- Robinson, A. R., and L. J. Walstad, Altimetric data assimilation for ocean dynamics and forecasting, *Johns Hopkins APL Tech. Dig.*, 8, 267–271, 1987.
- Tai, C.-K., Estimating the surface transport of meandering oceanic jet streams from satellite altimetry: surface transport estimates for the Gulf Stream and the Kuroshio Extension, *J. Phys. Oceanogr.*, in press, 1990.
- Tai, C.-K., and C. Wunsch, An estimate of global absolute dynamic topography, *J. Phys. Oceanogr.*, 14, 457–463, 1984.
- Tracey, K. L., and D. R. Watts, On Gulf Stream meander characteristics near Cape Hatteras, *J. Geophys. Res.*, 91, 7587–7602, 1986.

K. A. Kelly and S. T. Gille, Woods Hole Oceanographic Institution, Woods Hole, MA 02543.

(Received May 10, 1989;  
accepted July 10, 1989.)